Elevated temperature material behaviour of high strength steel

D. Winful[abc], K.A. Cashell[b], S. Afshan[b], A.M. Barnes[c] and R.J. Pargeter[c]

[a] National Structural Integrity Research Centre, Brunel University London and TWI, UK
[b] Brunel University London
[c] TWI, UK

Abstract:

This paper presents an experimental investigation into the behaviour of high strength steel structures (i.e. yield strength between 460 and 700 N/mm^2) in fire conditions. The paper proceeds with a description of the experimental programme that includes two different grades of high strength steel (HSS) with the aim of assessing (i) the mechanical properties at elevated temperature through tensile testing and (ii) the effect of chemical composition and processing route on the microstructure through a detailed metallurgical investigation. The investigation takes a holistic view of the analysis whereby the effect of processing route and composition on the microstructure and hence mechanical properties are assessed. In this paper, following a detailed description of the tests under isothermal conditions, the results are analysed to determine strength and stiffness reduction factors at elevated temperatures and these values are compared with literature and the design standards.

Keywords:
Fire engineering; Steel structures; Strength and testing of materials;

List of notation

A_0	elongation after fracture
A_c	cross-sectional area of the tensile specimen
d_o	diameter of tensile specimen in the gauge length
$E_{a,20}$	elastic modulus at ambient temperature (20°C)
$E_{a,\theta}$	elastic modulus at temperature θ
$f_{p,20}$	proportional limit at ambient temperature (20°C)
$f_{p,\theta}$	proportional limit at temperature θ
$f_{0.2p,20}$	0.2% proof strength at ambient temperature (20°C)
$f_{0.2p,\theta}$	0.2% proof strength at temperature θ
$f_{u,20}$	ultimate strength at ambient temperature
f_y	nominal or design yield strength
$f_{y,20}$	effective yield strength at ambient temperature θ (20°C)
$f_{y,\theta}$	effective yield strength at temperature θ
$k_{p,\theta}$	the reduction factor for the proportional limit at steel temperature θ
$k_{0.2p,\theta}$	the reduction factor for the 0.2% proof strength at steel temperature θ
$k_{y,\theta}$	the reduction factor for the effective yield strength at steel temperature θ
$k_{Ea,\theta}$	the reduction factor for Yong's modulus at steel temperature θ
L_c	parallel length of the tensile specimen
L_o	gauge length of tensile specimen
L_t	total length of tensile specimen

L_u	final gauge length of tensile specimen after fracture
$\varepsilon_{t,\theta}$	limiting strain for yield strength at temperature θ
$\varepsilon_{u,\theta}$	ultimate strain temperature θ
$\varepsilon_{y,\theta}$	yield strain (total strain at 2.0%) at temperature θ
θ	temperature

1   Introduction

During the conceptual design stage of a project, the selection of materials and structural schemes are often governed by the requirement for solutions to be economically viable whilst equally providing a positive contribution towards the environment and society. High strength steels (HSS), defined here as materials with yield strength between 460 and 700 N/mm² in accordance with EN 1993-1-12 (2007), have the potential to make a positive contribution towards these demands by reducing the material usage and hence weight of structural elements when employed in appropriate applications. Lighter structures can lead to smaller foundations, reduced transportation costs and potentially reduced construction times and costs, as well as lower CO_2 emissions and energy use during material production, transportation and construction. To date, the use of HSS in civil engineering has mainly been limited to specific applications such as offshore drilling rigs, heavy industrial plants, bridges and long span trusses. Their use in more common structural engineering applications is limited for a variety of reasons such as lack of reliable design guidelines, serviceability issues, the need for different welding procedures and misconceptions on the price/tonne (RFCS, 2014). Nevertheless, HSS are gaining increasing interest for civil engineering applications and there are a number of documented instances where HSS have been successfully utilised in structures. For example, the use of HSS in the Friends Arena Stadium in Solna, Sweden resulted in a structure 15% lighter when compared with using S355, €2.2 million savings in costs and 17% savings in greenhouse gas emissions (Ruukki, 2013). In addition, the use of HSS in the long span Oresund Bridge between Sweden and Denmark resulted in cost savings of more than €22 million (Rakshe, 2010).

One of the issues preventing more widespread use of HSS in structures is the lack of reliable information relating to the behaviour of these materials at elevated temperature. Although the Eurocode does include a section for HSS (EN 1993-1-12, 2007), the guidance for fire design is currently based on experiments on steel with yield strengths below 460 N/mm². This is partly due to the lack of test data available during the development of Eurocode 3 Part 1-12. For HSS, there are now limited data in the literature (e.g. Chen *et al.*, 2006; Qiang *et al.*, 2012; Choi *et al.*, 2014) that present the effects of temperature on the mechanical properties in terms of reduction factors. Whilst the loss of strength and stiffness during a fire is inevitable, the relationship between strength and stiffness of HSS at elevated temperature depends upon their inter-relationship with the alloying elements and processing route employed (Winful *et al.*, 2015). This suggests that by choosing particular alloying elements and processing routes, possible metallurgical effects such as secondary (or precipitation) hardening could potentially be utilised to delay the loss of strength and stiffness of HSS during a fire, therefore obtaining valuable evacuation time. However, because limited metallurgical analysis has been presented in the literature, the influence of strengthening mechanisms such as precipitation hardening on the performance of HSS at elevated temperature is not clear. Thus, although a primary aim of this work is to provide engineers and designers with essential and reliable mechanical property data to support the safe design of fire resistant structures made from HSS, a further objective is to develop a detailed understanding of the effects of steel

alloying and processing routes on the structural response of HSS in fire as these are likely to have a strong influence on the degradation of mechanical properties.

In this paper, a series of isothermal elevated temperature tests on two commercial HSS grades is described. Based on the findings of this study, data of the following mechanical properties are presented: proportional limit ($f_{p,\theta}$), 0.2% proof strength ($f_{0.2p,\theta}$), effective yield strength ($f_{y,\theta}$) based on the total strain level at 2% (in accordance with the Eurocode approach) and elastic modulus ($E_{a,\theta}$). The results are compared with available results in the literature and also the Eurocode curves (EN 1993-1-2, 2005).

2   Experimental investigation

Ambient and elevated temperature tensile tests were conducted on a Zwick Kappa 100 SS electromechanical testing machine, which has a maximum return speed of 100 mm/min. The machine consists of a load frame with a maximum capacity of 100 kN, a three-zone furnace with a temperature controller that has a maximum temperature capability of 1200 °C and testXpert II V3.6 software that monitors and controls the mechanical and thermal variables of the system through a digital closed loop control. A total of three K-type thermocouples was used to monitor the top, middle and bottom temperature of each tensile specimen. An axial contact extensometer with high purity alumina ceramic rods, compliant with ISO 9513 Class 1 (2012), was used to measure the strain (in the gauge length) up to 5% before switching to crosshead displacement to estimate the strain for the remainder of the test. The test set-up for one of the experiments is shown in Figure 1.

Table 1 presents the HSS grades which are included in the experimental investigation, covering a range of nominal yield strengths (f_y) between 690 and 700 N/mm^2 at ambient temperature (note that f_y is used to describe the nominal yield strength whilst $f_{y,\theta}$ is used to represent the effective yield strength in N/mm^2 defined in Section 2.5.3). The designations for structural steel grades within EN 10025 (2004) and EN 10149 (2013) are denoted by an S at the beginning followed by the nominal yield strength at ambient temperature and then the production route/delivery condition. Q in the designation S690QL refers to the quench and tempered production process whilst L indicates that the material meets the minimum impact energy requirement of 30 J at -40°C (2014). Likewise M and C in S700MC indicate thermo-mechanical control processed (TMCP) and cold-formed materials, respectively (2013).

The chemical compositions of the steels are presented in Table 2. As shown in this table, the quench and tempered steel A was alloyed with chromium (Cr), nickel (Ni), boron (B), and molybdenum (Mo) and was also microalloyed with titanium (Ti) and vanadium (V). Chromium is a hardening element while nickel provides toughness. Boron and molybdenum also add hardenability. Titanium and vanadium aid toughness and formability of the steel. The TMCP steel B (S700MC) had a lower carbon (C), and combined Cr, Ni, copper (Cu) and Mo content as well as a higher contribution of manganese (Mn) and combined microalloying with Ti, niobium (Nb) and V than steel A.

The tensile specimens were round with a diameter of either 6 mm (M10) or 8 mm (M12) in the gauge length L_o. M10 and M12 are the standard names of round tensile specimens and refer to the thread size of the tensile specimens (i.e. 10 and 12 mm, respectively). This was the maximum

standard size possible from each plate. They were machined parallel to the rolling direction from each of the plates detailed in Table 1. The dimensions of the specimens were specified in accordance with ISO 6892 Part 1 (2009) and Part 2 (2011), and are shown in Figure 2. The total length L_t, parallel length L_c and the diameter at three positions along the gauge length L_o were measured for each tensile specimen using a digitised travelling light microscope. The average diameter d_o was then calculated and used to determine the cross-sectional area A_c for each tensile specimen.

The standard gauge length was calculated using Eq. (1) for proportional tensile specimens. L_o was rounded to nearest multiple of 5 mm, as recommended in ISO 6892-1 (2009). Such approximation is only valid if the difference between the calculated gauge length and approximate gauge length is less than 10%. This was the case for both the M12 and M10 specimens whereby the approximate gauge length was 40 and 30 mm, respectively. Alternatively, for round tensile specimens, $A_c = \frac{1}{4}\pi d_o^2$, and so Eq. (1) can be approximated to 5 times the diameter ($5d_o$). The corresponding gauge length for the M12 and M10 specimens using this method is also 40 and 30 mm, respectively. The approximate gauge length was marked on the specimens using Vernier callipers and a lathe. Once the tests were completed, the final gauge length after fracture, L_u, was measured by carefully fitting back together the broken specimen and using a digitised travelling light microscope. The elongation after fracture, A_0, was then calculated using Eq. (2). In total, 30 specimens (15 for each steel type) were tested in the current study.

$$L_o = 5.65 \sqrt{A_c} \tag{1}$$

$$A_0 = \frac{L_u - L_o}{L_o} \times 100 \tag{2}$$

3 Ambient temperature test programme

A total of six tensile tests (three for each of steels A and B) were conducted at ambient temperature in order to generate baseline room temperature tensile data. These were completed based on the recommendations given by Huang and Young (2014), including using the recommended strain rates, which are significantly lower than those presented in the ISO standards (ISO 6892-1, 2009). It was found that more data points are required in the elastic range in order to obtain an accurate value for the initial elastic modulus. The strain rates used in the current test programme are presented in Table 3.

For the ambient temperature tests, conventional strain gauges were used which could measure strains up to around 2% before debonding occurred. In each test two linear strain gauges were attached to the midpoint of each tensile specimen to verify the accuracy of the readings from the extensometer. An example of this comparison is shown in Figure 3. Generally there was good agreement between the measured elastic modulus from the strain gauge and the extensometer.

The values measured in the tests include the proportional limit ($f_{p,20}$) defined as the point where the stress-strain response changes from being linear to non-linear, the 0.2% proof strength ($f_{0.2p,20}$),

defined as the point where the initial elastic modulus offset at 0.2% strain intersects the stress-strain curve, the effective yield strength ($f_{y,20}$) typically defined as the point where the total strain at 2% intercepts the stress-strain curve, the ultimate strength ($f_{u,20}$) is defined as the maximum tensile strength measured and the elastic modulus ($E_{a,20}$).

Table 4 presents the data obtained from the tensile tests for each material along with the coefficient of variation COV, which is defined as a ratio of the standard deviation over the mean value from the three tests. The COV demonstrates good repeatability between the tests for both steels. For steel A (S690Q) the proportional limit and the elastic modulus had the highest COV at 1.6% and 1.4% respectively, whilst for steel B (S700MC) the COV for the proportional limit was 2.0%. Steel B (S700MC) had the highest strengths and elastic modulus but lower proportional limit and ductility compared to steel A (S690QL). The stress-strain curves are discussed further in Section 5.

4 Elevated temperature test programme

4.1 General

Tensile testing at elevated temperature may be conducted isothermally or anisothermally which are also known as steady-state and transient testing, respectively. In an isothermal test, the temperature of the specimen is equilibrated at the target temperature before straining to failure at a controlled rate. Isothermal tests can also be performed under a controlled stress rate although this method is seldom used because the softening part of the stress-strain diagram is not obtained (Dotreppe, 1997). In an anisothermal test, the specimen is held at a target tensile load and then the temperature is increased at a controlled rate until failure occurs. The total strain is recorded as a function of temperature θ and this can be converted into stress-strain curves (Figure 4) once the effect of thermal expansion has been removed from the data using the appropriate coefficient of thermal expansion.

There has been considerable discussion in the research community regarding the most representative test method for real fire conditions. Testing under isothermal conditions is more commonly used by researchers as it is easier to conduct and continuous stress-strain curves are produced directly, which can be favourable for complex structural fire resistance analysis (Chiew *et al.*, 2014). Moreover, the conditions are easier to control, compared with anisothermal testing and therefore comparison between results is more reliable. However, anisothermal tests are considered to be more representative of the conditions that steel members may experience during a fire, as creep effects are implicitly taken into account (Wang *et al.*, 2012).

Creep is a time dependent deformation that occurs when a material is subjected to a load, lower than that which causes yielding (Kodur and Dwaikat, 2010). The rate of creep increases with load and temperature and the influence of creep in steels are particularly evident at temperatures above 400°C (Anderberg, 1988). As creep is time dependent, it should be noted that it is a significant concern for insulated steel members, as they are generally heated at a slower rate (e.g. 5°C/min) compared with un-insulated elements. Therefore, the member is exposed to a given temperature window for longer periods of time leading to a greater influence of creep (Kodur and Dwaikat, 2010). This effect has been observed in the literature (e.g. Rubert and Schaumann, 1986; Anderberg 1988; Kirby and Preston, 1988), whereby heating rates below 5°C/min in anisothermal tests resulted in

lower limiting temperatures at which anticipated failure is expected to occur. In practice, this failure corresponds to when the strain approaches values corresponding to the limits of deflection or instability under fire conditions (Kirby and Preston, 1988). Creep is not commonly considered to contribute to isothermal test results, but a slow strain rate will allow some creep to occur, and a lower effective yield strength has been reported at lower strain rate (Anderberg, 1988; Outinen, 2007; Knobloch *et al.*, 2013). The choice of strain rate is not currently correlated to fire resistance in the European structural fire design guidelines and so researchers have tended to use the values specified in other standards (e.g. ISO 6892-2, 2011; ASTM E21-09, 2009), when conducting tensile tests under isothermal conditions.

For large strains (i.e. >2 %), the influence of creep on the overall fire resistance period has been found to be within the reasonable error band for elevated temperature tensile testing and therefore, it has been suggested that the effect of creep can be ignored (Twilt, 1988). On the other hand, Kodur and Dwaikat (2010) found that neglecting high temperature creep in fire resistance analysis may lead to unconservative fire resistance predictions, particularly for restrained elements. However, for unrestrained elements, the data obtained from isothermal testing is deemed to be satisfactory.

The current programme of testing includes samples tested under isothermal testing conditions. The specimens were heated to a target temperature of 100, 200, 300, 400, 500, 600, 700 and 800°C and repeat tests were conducted at 100, 400, 500 and 600°C. For the tests at elevated temperature, strain gauges were not employed. This is because they tend to debond during the heating process prior to the tensile load being applied due to the mismatch in coefficient of thermal expansion between the adhesive and the surface of the specimen and/or the strain gauge (Gales *et al.*, 2012; Motra *et al.*, 2014). Conventional strain gauges are also temperature sensitive resulting in less reliable measurement with increasing temperature. Alternative methods for measuring the strain at elevated temperature include costly specialist strain gauges and adhesives, digital image correlation (DIC) and a contact extensometer (Gales *et al.*, 2012). In this investigation, a contact extensometer was used to measure the strain up to around 5% at which point the extensometer was removed to avoid any damage occurring; at higher strains, the (estimated) extension was measured using the crosshead displacement. The most influential experimental parameters in terms of their impact on the results are the strain and heating rates employed and these are discussed in more detail hereafter.

4.2 Strain rate

As mentioned above, the rate at which strain in the specimen is increased during elevated temperature tensile testing has been found to influence the final results (Knobloch *et al.*, 2013). In tests on mild steel (S355) at 400, 550 and 700°C under isothermal conditions, the reduction factors from the experimental data did not correlate well with the European and American fire design guidelines when the strain rate was 0.0002/min or 0.001/min which, based on the concept of reaching the "runaway" strain at 2% total strain, correspond to durations of 100 and 20 minutes, respectively. There was however, good agreement between the experimental data and the reduction factors when the strain rate was 0.005/min. A strain rate of 0.005 ± 0.002/min was adopted throughout the current investigation in order to be consistent with the standards (ISO 6892-2, 2011; ASTM E21-09, 2009) and other researchers (e.g. Chen *et al.*, 2006; Qiang *et al.*, 2012).

4.3 Heating rate

In structural fire design, heating rates for steel should be within the range of 2 to 50°C/min as specified in EN 1993-1-2 (2005) in order to reflect real fire behaviour. Typically, a rate of 3°C/min is representative of a heavily insulated steel member in a typical building fire whilst 50°C/min is more characteristic of a non-insulated steel member (Twilt, 1988). A heating rate of 10°C/min, which represents a fully loaded steel member surviving for approximately 1 hour in accordance with the ISO 834 standard fire resistant tests (ISO, 1999), has been regularly used in literature (e.g. Kirby and Preston, 1988; Choi *et al.*, 2014). Heating rates in isothermal tests need to be controlled to ensure uniform and stable temperature distribution, in a time frame that does not allow any significant change in microstructure or properties to occur. In this study, the heating rates used are shown in Table 5. In cases where the target temperature was greater than 400°C, a rate of 10°C/min was employed although this was reduced to 3°C/min when the temperature reached 80% of the target value in order to avoid temperature overshoot and to ensure the prescribed temperature was reached within the limits of ±3°C. This ensured that the entire parallel length of the specimen reached thermal equilibrium by the time the target temperature was achieved. Tests conducted at 100, 200, 300 and 400°C took approximately one hour to reach, and stabilise at, the target temperature. Once the target temperature was reached, the specimen was held at that temperature for at least fifteen minutes in order to ensure that the whole specimen was in thermal equilibrium. At such temperatures, a one hour heating time has a minimal effect on the strength or stiffness, as limited microstructural effects would be expected (Smith *et al.*, 1981).

4.4 Key parameters measured during testing

At elevated temperature, the yield strength becomes increasingly difficult to quantify because of the large strains exhibited and material nonlinearity. Eurocode 3 Part 1-2 (2005) idealises the stress-strain response at elevated temperature as illustrated in Figure 5. The response is assumed to be linear up to the proportional limit ($f_{p,\theta}$) and this is followed by an elliptical representation until the maximum stress ($f_{y,\theta}$) is achieved at a strain of $\varepsilon_{y,\theta}$, where $\varepsilon_{y,\theta}$ is commonly defined as the total strain level at 2.0 % (Wang *et al.*, 2012). Following this, a constant strength is assumed between $\varepsilon_{y,\theta}$ and the limiting strain ($\varepsilon_{t,\theta}$) before the stress drops to zero at the ultimate strain ($\varepsilon_{u,\theta}$).

5 Stress–strain curves

The engineering stress-strain curves obtained from isothermal tests conducted at temperatures between 20 and 800°C are shown in Figure 6 for steel A (S690QL) and Figure 7 for steel B (S700MC) where part (a) of each figure presents the full response whilst part (b) shows a closer view of the low-strain range. General observations are that as the temperature increases it becomes harder to distinguish between the linear and non-linear portion of the curves as the linear elastic part of the stress-strain curve decreases. This is particularly true for steel A (S690QL). Steel B (S700MC) has a more rounded stress-strain curve with no distinct yield point at 20°C.

6 Reduction factors

Reduction factors are typically used to express how the strength and stiffness properties degrade with increasing temperature and are defined as the ratio between the mechanical property being considered at elevated temperature and the equivalent value at ambient temperature. The

acceptance criteria for structural steel components at elevated temperature are set to ensure that the structural integrity is maintained for a sufficient period of time to allow for safe evacuation. The criteria are commonly defined as a minimum temperature (typically 550°C) at which the reduction factor is 0.6, or when a limiting strain or deflection has been reached (Billingham *et al.*, 2003) Alternatively performance may be required to exceed a reduction curve over the temperature range.

In this section, the main parameters related to strength and stiffness (i.e. $f_{p,\theta}$, $f_{0.2p,\theta}$, $f_{y,\theta}$ and $E_{a,\theta}$) are assigned reduction factors based on the test data. The results presented in Table 6 are later compared with published data where tests were similarly conducted under isothermal conditions (i.e. Chen *et al.*, 2006; Qiang *et al.*, 2012; Choi *et al.*, 2014) and the design curves given in EN 1993-1-2 (2005).

6.1   Proportional limit

As stated previously, the proportional limit ($f_{p,\theta}$) is defined as the point where the stress-strain response changes from being linear to non-linear. This was determined as the point where the stress-strain curve deviates from the initial elastic modulus. The rationale for introducing the proportional limit values into the Eurocodes at elevated temperatures was to capture the viscoelastic behaviour, which is partly due to creep (Kodur *et al.*, 2010). Figure 8 shows the reduction factors of the proportional limit (i.e. $k_{p,\theta} = f_{p,\theta}/f_{y,20}$) together with similar results from another test programme (i.e. Choi *et al.*, 2014) and EN 1993-1-2 (2005). From Figure 8 it can be seen that at low levels of elevated temperature (i.e. 20-300°C), the reduction factors provided in the code are unconservative. The standard predicts that the material will have greater strength retention than indicated by the test results. The Eurocode assumes that at 20 and 100°C the stress-strain curve is perfectly bilinear, meaning that the steel behaves in a linear-elastic manner up to the proportional limit and then exhibits a yield plateau such that $f_{p,\theta} = f_{y,\theta}$. However, for both steels A (S690QL) and B (S700MC), the stress-strain curve is not perfectly bilinear at 20 and 100°C, especially for steel B (S700MC) where no distinctive yield point was observed (see Figure 7). Above 300°C for steels A (S690QL) and HSA800 (as discussed by Choi et al. (2014)), and 400°C for steel B (S700MC), the reduction factors provided in the code are conservative and are shown to provide a good representation of the behaviour.

6.2   0.2% proof stress

As the yield stress is difficult to identify in materials with a non-linear stress-strain response where no distinctive yield point is observed (e.g. TMCP steel and stainless steel), the yield strength at ambient temperature is usually defined in terms of a proof stress at a particular offset strain, typically 0.2% strain. The 0.2% proof stress is often used in the design of class 4 (slender) steel members, where local buckling will occur before the yield strength is reached in one or more parts of the cross-section (EN 1993-1-1, 2005). Accordingly, in Figure 9, the reduction values for the 0.2% proof strength at elevated temperatures (i.e. $k_{0.2p,\theta} = f_{0.2p,\theta}/f_{0.2p,20}$) are presented along with data from the literature (i.e. Chen *et al.*, 2006; Qiang *et al.*, 2012; Choi *et al.*, 2014) and the figures determined using Annex E of the Eurocode (EN 1993-1-2, 2005). From Figure 9, it can be seen that generally, the reduction factors provided in the Eurocode are conservative at temperatures greater than 100°C, with the exception of S690QL tested by Qiang *et al.* (2012) at 700°C. At temperatures below 100°C the $k_{0.2p,\theta}$ reduction factors from the Eurocode are unconservative and do not depict the loss in strength accurately. Only HSA800 tested by Choi *et al.* (2014) met or exceeded the $k_{0.2p,\theta}$ reduction factors from the Eurocode at all temperatures.

6.3   Effective yield strength

In Eurocode 3 Part 1-2 (2005), the effective yield strength at elevated temperature ($f_{y,\theta}$) is defined as the stress level at which the stress-strain curve is truncated to provide a yield plateau, as shown earlier in Figure 5. In practice, this has been consistently based on the total strain level at 2.0%, which is a high working strain for structural steels at ambient temperature (Wang *et al.*, 2012) but in a fire scenario, large strains are accepted as it is assumed that structural members are likely to be either repaired or replaced once exposed to the fire (Gardner *et al.*, 2016). Figure 10 presents the reduction factors for the effective yield strength at elevated temperatures (i.e. $k_{y,\theta} = f_{y,\theta}/f_{y,20}$) for a range of temperatures, which are presented together with data from the literature (i.e. Chen *et al.*, 2006; Qiang *et al.*, 2012; Choi *et al.*, 2014) as well as the reduction curve taken from the Eurocode (EN 1993-1-2, 2005).

Generally, it is observed that the Eurocode provides a reasonable and conservative prediction for the effective yield strength for steel A (S690QL) and steel B (S700MC) with the exception of between 100 and 400°C for steel A (S690QL) and between 100 and 200°C for steel B (S700MC). However, the Eurocode is shown to provide unconservative reduction factors for the effective yield strength compared with the values tested and reported in the literature, with the exception of HSA800 tested by Choi *et al.* (2014) at 300°C and BISPLATE 80 (S690Q) tested by Chen *et al.* (2006) between 500 and 700°C. Both steel A (S690QL) and B (S700MC) demonstrate better strength reduction factors from 500 to 800°C than the steels from literature. Steel B, a thermomechanical control processed material had the better strength reduction properties compared to steel A (S690QL) at all tested temperatures. This steel contains niobium and titanium and also had the highest reported vanadium content of the tested steels (see Table 2) which suggests that this steel may contain a stable, fine dispersion of niobium or vanadium carbonitrides, or even form these as the temperature increases. Such precipitates play a crucial role in retention of steel strength at temperatures up to 650°C (Sha *et al.*, 1999).

6.4   Elastic modulus

The elastic modulus is a very important property in structural engineering as it is used to determine the stiffness of a structural element and hence its buckling resistance. The elastic modulus at ambient and an elevated temperature θ (i.e. $E_{a,20}$ and $E_{a,\theta}$, respectively) were determined from the test results based on the tangent of the initial linear elastic region of the stress-strain curve (Figure 5). Figure 11 illustrates the reduction factors determined from the test programme (i.e. $k_{E,\theta} = E_{a,\theta}/E_{a,20}$) and compares these with equivalent values taken from the literature (i.e. Chen *et al.*, 2006; Qiang *et al.*, 2012; Choi *et al.*, 2014) and the Eurocode (EN 1993-1-2, 2005). In Eurocode 3 Part 1-2 (2005), the reduction factors for elastic modulus decrease more rapidly than those for $f_{y,\theta}$, suggesting that the failure mode of a steel member may change at elevated temperature. For example, a steel member that is designed to fail under overload by reaching its strength limit at ambient temperature may experience buckling failure at elevated temperature in certain cases. This is likely to be especially important for HSS structures as these members tend to be made from more slender elements compared to members made from normal strength steel and so stability calculations are often critical. Therefore, any potential retardation in the reduction in the loss of stiffness with increasing temperature is positive for HSS applications.

From the results presented in Figure 11, it can be seen that the elastic modulus for steels A and B follows a similar trend to those in the published literature (i.e. Chen *et al.*, 2006; Qiang *et al.*, 2012;

Choi *et al.*, 2014) and the reduction factors are generally rather conservative with the exception of steel A (S690QL) at 100°C and steel B (S700MC) at 100 and 200°C. At higher temperatures, above 200°C, the results from this test programme and literature suggest that the current reduction curves in the Eurocode for HSS are overly conservative and do not allow the good stiffness retention properties of these materials to be exploited in design. There is certainly evidence in the figure that would support less conservative and more attractive reduction factors being proposed for the next edition of the Eurocode for HSS, once more experimental validation is available.

7   Conclusions

The proportional limit ($f_{p,\theta}$), 0.2% proof strength ($f_{0.2p,\theta}$), effective yield strength ($f_{y,\theta}$) and elastic modulus ($E_{a,\theta}$) were obtained from ambient and isothermal tests on two commercially available HSS (S690QL and S700MC) at temperatures between 20 and 800°C. The results were presented as reduction factors, where data was normalised by the measured property at ambient temperature and compared to literature (Chen *et al.*, 2006; Qiang *et al.*, 2012; Choi *et al.*, 2014) and Eurocode 3 Part 1-2 (2005). The results suggest that the Eurocode provides conservative predictions for the proportional limit at temperatures greater than 300°C and the elastic modulus at all temperatures apart from 100°C for the steels tested. Steel B (S700MC) had the best strength and stiffness reduction factors compared with steel A (S690Q) and it is clear from the results presented in Table 2 and Table 6 that there are significant differences in the performances of high strength steels from different sources. It is clear that the chemical composition and production route are influential to the material performance at elevated temperatures and this is an area that requires further research.

Acknowledgements

References

Anderberg, Y. (1988). Modelling Steel Behaviour. Fire Safety Journal. 13: 17–26.

ASTM E21-09 (2009). Standard Test Methods for Elevated Temperature Tension Tests of Metallic Materials. ASTM International, West Conshohocken, PA, USA.

Billingham, J., Sharp, J. V., Spurrier, J., Kilgallon, P.J. (2003) Review of the performance of high strength steels used offshore. Health Saf. Exec, 11.

EN 10025-6 (2004). Hot rolled products of structural steels - Part 6: Technical delivery conditions for flat products of high yield strength structural steels in the quenched and tempered condition. BSI, London, UK.

EN 10149-2 (2013). Hot rolled flat products made of high yield strength steels for cold forming Part 2 : Technical delivery conditions for thermomechanically rolled steels. BSI, London, UK.

EN 1993-1-1 (2005). Eurocode 3. Design of steel structures - Part 1-1: General rules and rules for buildings. CEN, Brussels.

EN 1993-1-2 (2005). Eurocode 3: Design of steel structures - Part 1-2: General rules - Structural fire design. CEN, Brussels.

EN 1993-1-12 (2007). Eurocode 3: Design of steel structures - Part 1-12 - Additional rules for the extension of EN 1993 up to steel grades S 700. CEN, Brussels.

Chen, J., Young, B., Uy, B. (2006) Behavior of high strength structural steel at elevated temperatures Journal of Structural Engineering. 132 (12): 948–1954.

Chiew, S.P., Zhao, M.S., Lee, C.K. (2014) Mechanical properties of heat-treated high strength steel under fire/post-fire conditions. Journal of Constructional Steel Research. 98: 12–19.

Choi, I.-R., Chung, K.-S., Kim, D.-H. (2014) Thermal and mechanical properties of high-strength structural steel HSA800 at elevated temperatures. Materials and Design. 63: 544–551.

Cooke, G.M.E. (1988) An introduction to the mechanical properties of structural steel at elevated temperatures. Fire Safety Journal. 13(1): 45–54.

Dotreppe, J.C. (1997) Mechanical properties of quenched and self-tempered reinforcing steel at elevated temperatures compared with recommendations of Eurocode 2-Part 1–2. Materials and Structures. 30(7): 430–438.

Gales, J.A., Bisby, L.A., Stratford, T. (2012) New parameters to describe high-temperature deformation of prestressing steel determined using digital image correlation. Structural Engineering International: Journal of the International Association for Bridge and Structural Engineering (IABSE). 22(4): 476–486.

Gardner, L., Bu, Y., Francis, P., Baddoo, N.R., Cashell, K.A., McCann, F. (2016) Elevated temperature material properties of stainless steel alloys. Journal of Constructional Steel Research. 114: 977–997.

Huang, Y., Young, B. (2014) The art of coupon tests. Journal of Constructional Steel Research. 96: 159–175.

ISO 834-1 (1999). Fire resistance tests— elements of building construction. Part 1: general requirements. International Standards Organisation.

ISO 6892-1 (2009). Metallic materials - Tensile Testing Part 1: Method of test at ambient temperature. International Standards Organisation.

ISO 6892-2 (2011). Metallic materials - Tensile testing Part 2: Method of test at elevated temperature. International Standards Organisation.

ISO 9513 (2012). Metallic materials - Calibration of extensometer systems used in uniaxial testing. International Standards Organisation.

Kirby, B.R., Preston, R.R. (1988) High Temperature Properties of Hot-rolled , Structural Steels for Use in Fire Engineering Design Studies. Fire Safety Journal. 13: 27–37.

Knobloch, M., Pauli, J., Fontana, M. (2013) Influence of the strain-rate on the mechanical properties of mild carbon steel at elevated temperatures. Materials and Design. 49: 553–565.

Kodur, V.K.R., Dwaikat, M.M.S., Fike, R. (2010) High temperature properties of steel for fire resistance modeling of structures. Journal of Materials in Civil Engineering. 22 (5): 423–434.

Kodur, V.K.R., Dwaikat, M.M.S. (2010) Effect of high temperature creep on the fire response of restrained steel beams. Materials and Structures. 43(10): 1327–1341.

Luecke, W.E., McColskey, J.D., McCowan, C.N., Banovic, S.W., Fields, R.J., Foecke, T., Siewart, T.A., Gayle F.W. (2005) Federal Building and Fire Safety Investigation of the World Trade Center Disaster: Mechanical Properties of Structural Steels. NIST NCSTAR1-3D, National Institue of Standards and Technology, Gaithersburg, MD, USA

Motra, H.B., Hildebrand, J., Dimmig-Osburg, A. (2014) Assessment of strain measurement techniques to characterise mechanical properties of structural steel. Engineering Science and Technology, an International Journal. 17(4): 260–269.

Outinen, J. (2007) Mechanical properties of structural steels at high temperatures and after cooling down. Helsinki University of Technology Laboratory of Steel Structures publications, Teknillisen korkeakoulun teräsrakennetekniikan laboratorion julkaisuja, 32.

Pauli, J., Somaini, D., Knobloch, M., Fontana, M. (2012) Experiments on steel under fire conditions. Swiss Federal Institute of Technology Zurich, Institute of Structural Engineering.

Qiang, X., Bijlaard, F., Kolstein, H. (2012) Dependence of mechanical properties of high strength steel S690 on elevated temperatures. Construction and Building Materials. 30: 73–79.

Rakshe, B. (2010) Modern high strength Nb-bearing structural steels. Millenium Steel India. pp. 69–72.

Research Fund for Coal and Steel (RFCS) of the European Commission (2014) Summaries of RFCS Projects 2003 – 2014 Full list of projects co-financed by the Research Fund for Coal and Steel of the European Commission, pp. 565 and 569

Rubert, A., Schaumann, P. (1986) Structural steel and plane frame assemblies under fire action. Fire Safety Journal. 10(3): 173–184.

Ruukki (2013) High-strength special steels create new architecture. [Online]. Available from: http://www.ruukki.com/News-and-events/News-archive/2013/High-strength-special-steels-create-new-architecture [Accessed: 27 April 2015].

Sha, W., Kelly, F.S., Guo, Z. (1999) Microstructure and properties of nippon fire-resistant steels. Journal of Materials Engineering and Performance. 8(5): 606–612.

Smith, C.I., Kirby, B.R., Lapwood, D.G., Cole, K.J., Cunningham, A.P., Preston, R.R. (1981) The reinstatement of fire damaged steel framed structures. Fire Safety Journal. 4(1): 21–62.

Twilt, L. (1988) Strength and deformation properties of steel at elevated temperatures: Some practical implications. Fire Safety Journal. 13: 9–15.

Wang, Y.C., Burgess, I.W., Wald, F., Gillie, M. (2012) Performance-based fire engineering of structures. CRC Press.

Winful, D.A., Cashell, K.A., Barnes, A.M., Pargeter, R.J. (2015) High Strength Steel in Fire. In Proceedings of the First International Conference on Structural Safety under Fire and Blast CONFAB 2015. Glasgow, UK, pp. 105–114.

Table 1 Grades of commercial HSS included in the programme

	Grade	f_y (N/mm^2)	Nominal plate thickness (mm)	Tensile specimen	Manufacturing process
Steel A	S690QL	690	16	M12	Quenched and tempered
Steel B	S700MC	700	12	M10	TMCP + cold-formed

Table 2 Chemical composition of the HSS included in the programme

	Chemical composition (wt %)											
	C	Si	Mn	Cr	Ni	Cu	Mo	Al	Ti	Nb	V	B
Steel A	<0.20	<0.5	<1.60	≤1.50	≤2.10	≤0.55	<0.60	<0.040	<0.05	-	<0.10	<0.0050
Steel B	<0.08	<0.2	<2.00	♦	♦	♦	residual	<0.050	<0.15*	≤0.09*	≤0.20*	-

*Ti + Nb +V < 0.22%

♦Cr + Ni + Cu < 0.5

Table 3 Strain rates used in testing

Strain (%)	Strain rate (/min)
0 – 0.2	0.0009
0.2 – fracture	0.0070

Table 4 Mechanical properties of steel A and B at ambient temperature

	Steel A (S690Q)					Steel B (S700MC)				
	Test			Avg	COV	Test			Avg	COV
	1	2	3			1	2	3		
$f_{p,20}$ (N/mm^2)	600.0	580.0	600.0	593.3	1.6%	415.0	410.0	430.0	418.3	2.0%
$f_{0.2p,20}$ (N/mm^2)	706.0	706.0	707.0	706.3	0.1%	752.0	746.0	750.0	749.3	0.3%
$f_{y,20}$ (N/mm^2)	742.8	737.3	737.9	739.3	0.3%	802.1	799.3	800.7	800.7	0.1%
$f_{u,20}$ (N/mm^2)	783.4	791.7	800.4	791.8	0.9%	838.0	833.7	837.3	836.3	0.2%
$E_{a,20}$ (GPa)	203.2	197.3	197.3	199.3	1.4%	224.6	225.8	223.6	224.7	0.4%

Table 5 Heating rates used in this experimental programme

Target temperature (°C)	Heating rate (°C/min)
100	2
200	3
300	5
>400	10

Table 6 Reduction factors for strength and stiffness

θ, Temperature (°C)	Steel A (S690Q)				Steel B (S700MC)			
	$f_{p,\theta}/f_{y,20}$	$f_{0.2p,\theta}/f_{0.2p,20}$	$f_{y,\theta}/f_{y,20}$	$E_{a,\theta}/E_{a,20}$	$f_{p,\theta}/f_{y,20}$	$f_{0.2p,\theta}/f_{0.2p,20}$	$f_{y,\theta}/f_{y,20}$	$E_{a,\theta}/E_{a,20}$
20	0.80	1.00	1.00	1.00	0.52	1.00	1.00	1.00
100*	0.73	0.98	0.97	0.95	0.60	0.99	0.97	0.91
200	0.73	0.95	0.95	0.96	0.60	0.94	0.94	0.97
300	0.66	0.92	0.97	0.92	0.57	0.98	1.02	0.94
400*	0.62	0.91	0.93	0.89	0.45	0.92	0.99	0.91
500*	0.47	0.80	0.84	0.89	0.44	0.81	0.86	0.85
600*	0.41	0.63	0.66	0.75	0.39	0.68	0.71	0.79
700	0.16	0.32	0.34	0.38	0.24	0.47	0.45	0.63
800	0.06	0.10	0.11	0.27	0.14	0.23	0.21	0.39

*repeated tests
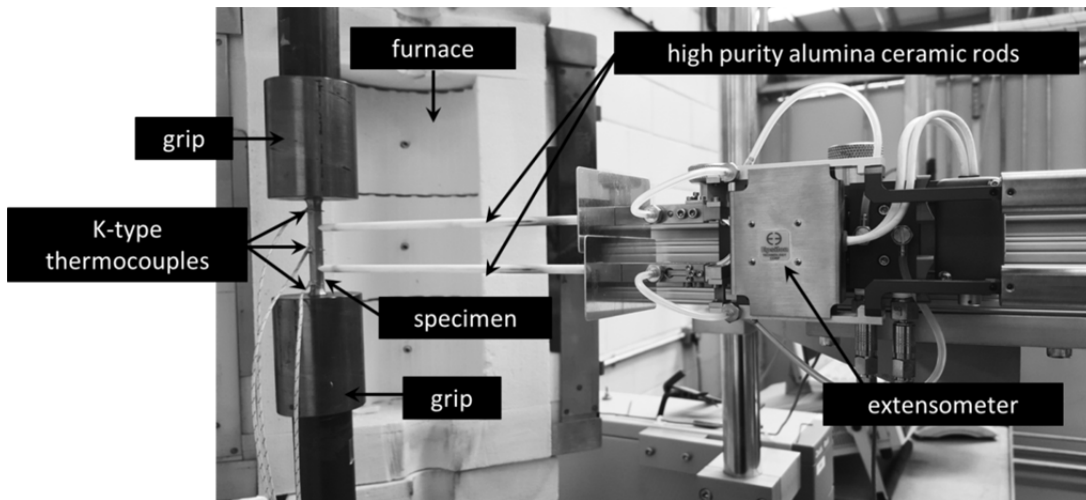
Figure 1: Experimental set–up (furnace open)

<div align="center">(a)</div>
<div align="center">(b)</div>
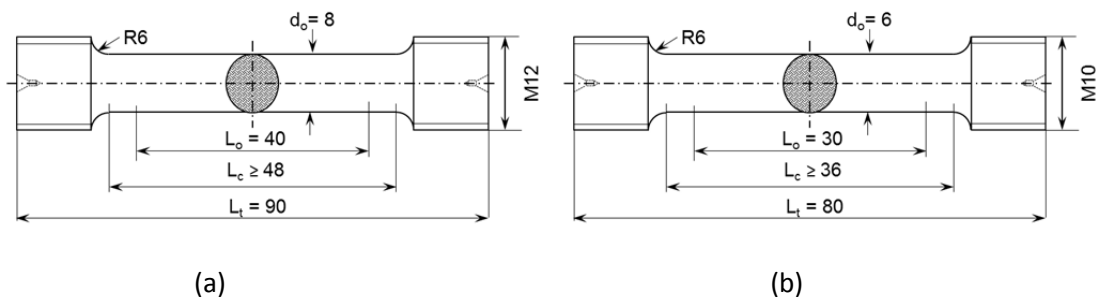
Figure 2: Dimensions of a (a) M12 and (b) M10 tensile specimen (all measurements are in *mm*)
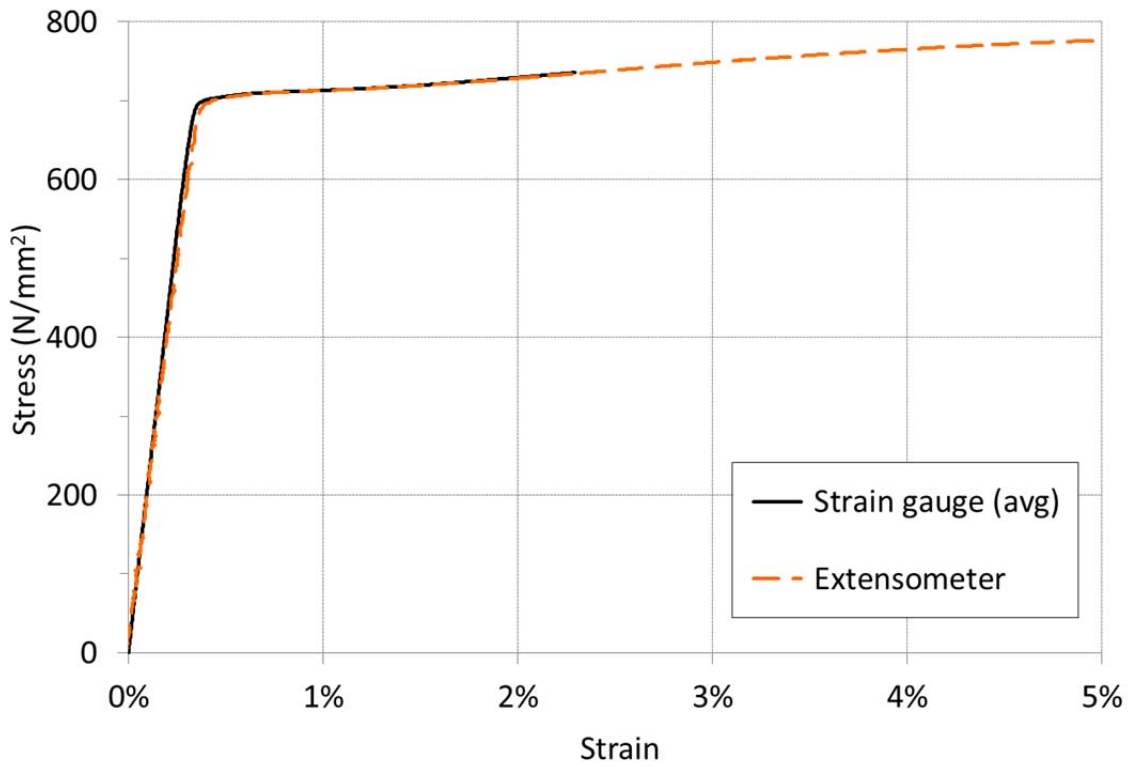
Figure 3: Comparison between strain measurements for steel A (S690QL) obtained from the average of two strain gauges and an extensometer
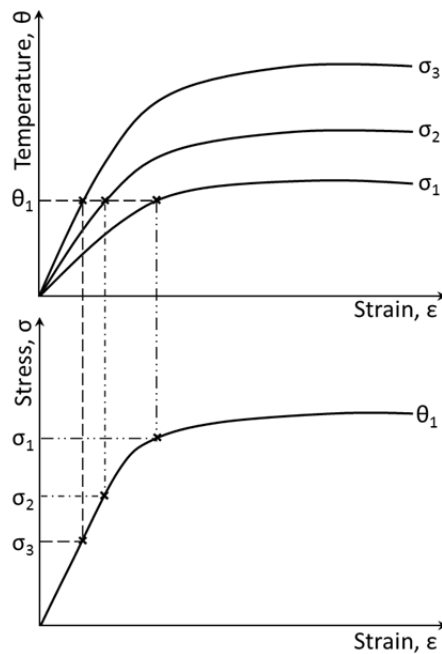
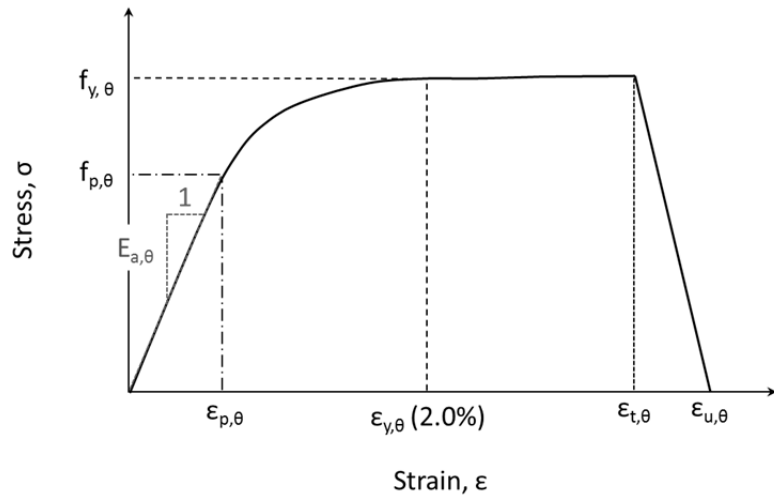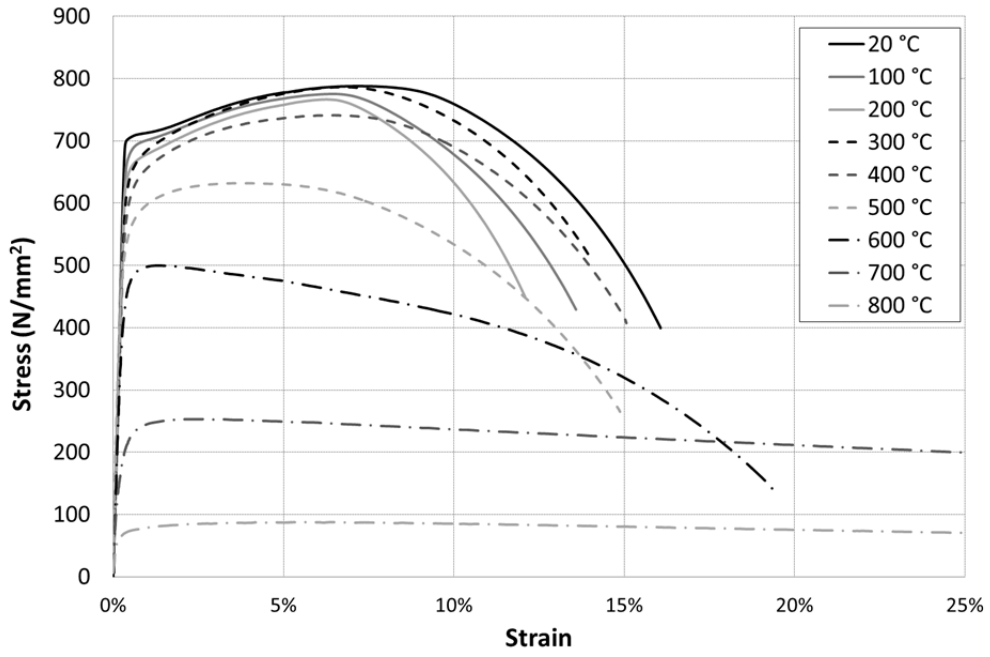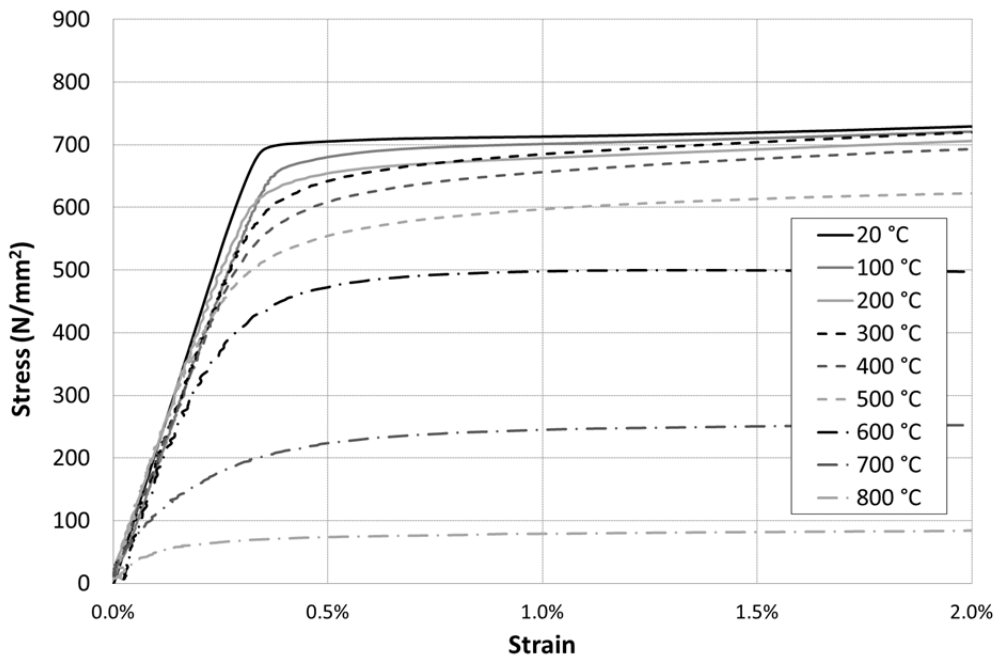**Figure 4: Converting temperature-strain curves from transient test result into stress-strain curves**

Figure 5: Idealised stress–strain curve at elevated temperature adopted from EN 1993-1-2 (2005)

(a)

(b)

Figure 6: Engineering stress-strain curves for steel A (S690QL) from 20 to 800°C (a) up to 25% strain and (b) up to 2% strain
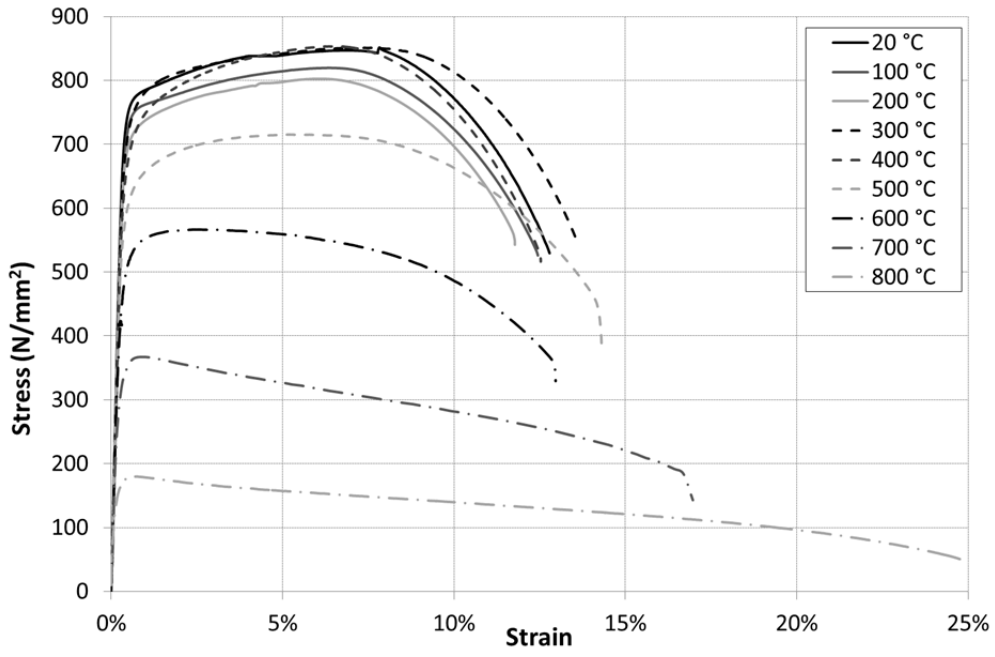
(a)
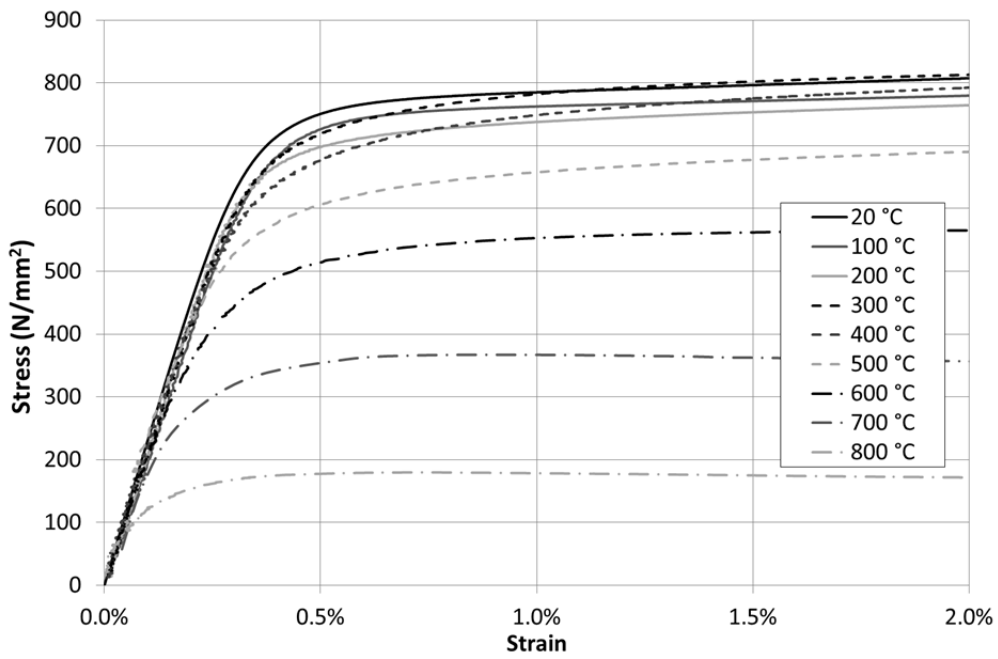
(b)

Figure 7: Engineering stress-strain curves for steel B (S700MC) from 20 to 800°C (a) up to 25% strain and (b) up to 2% strain
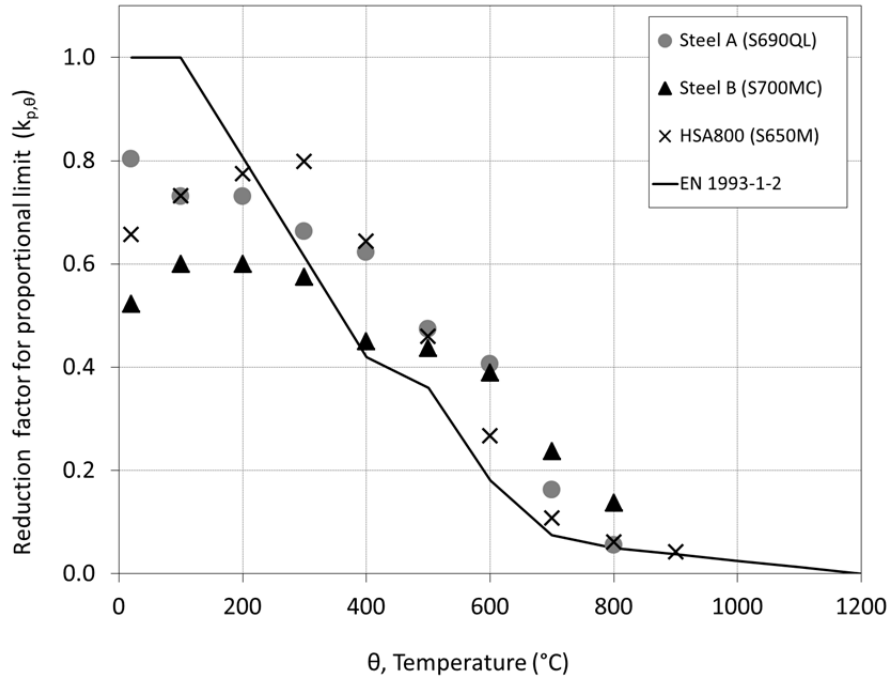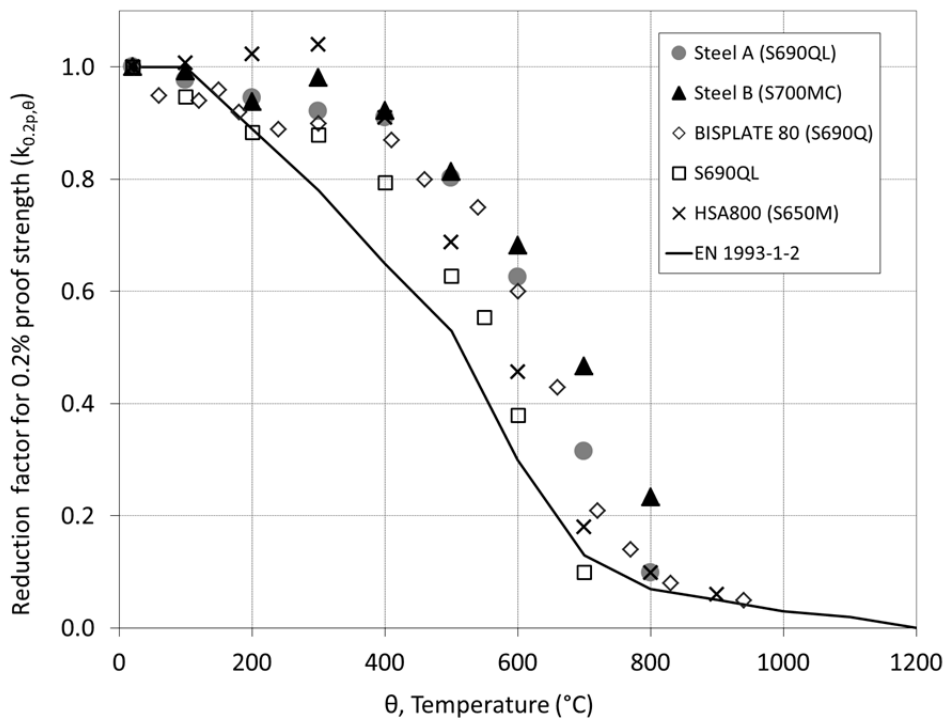
Figure 8: Reduction factors for the proportional limit

Figure 9: Reduction factors for the 0.2% proof strength
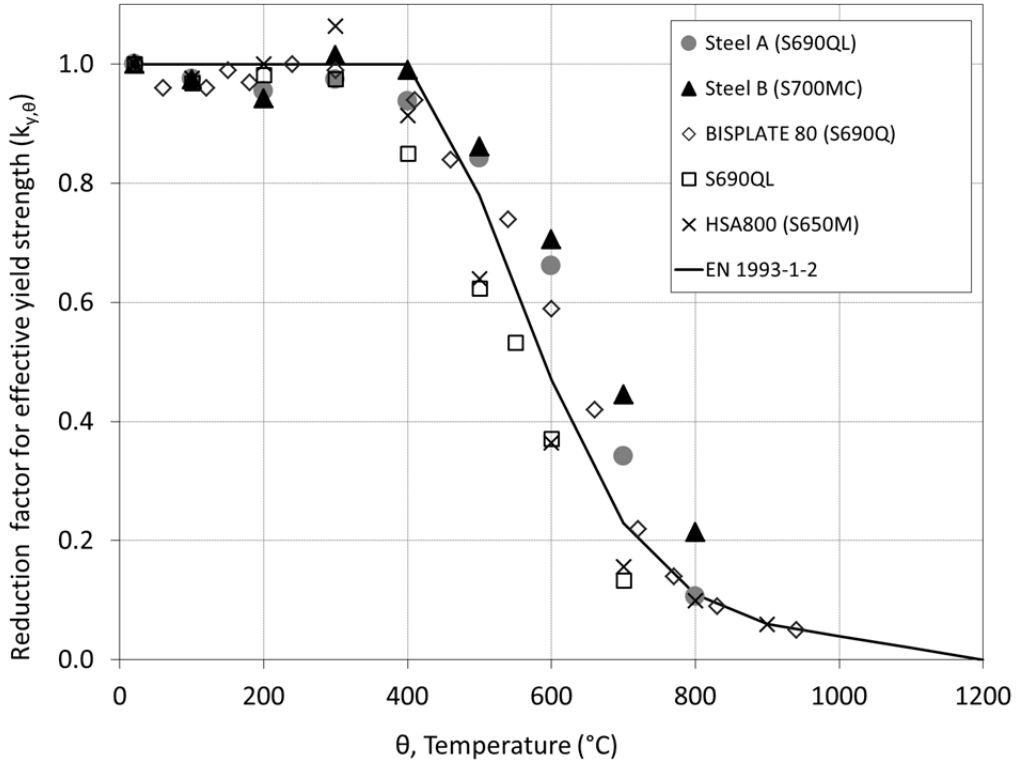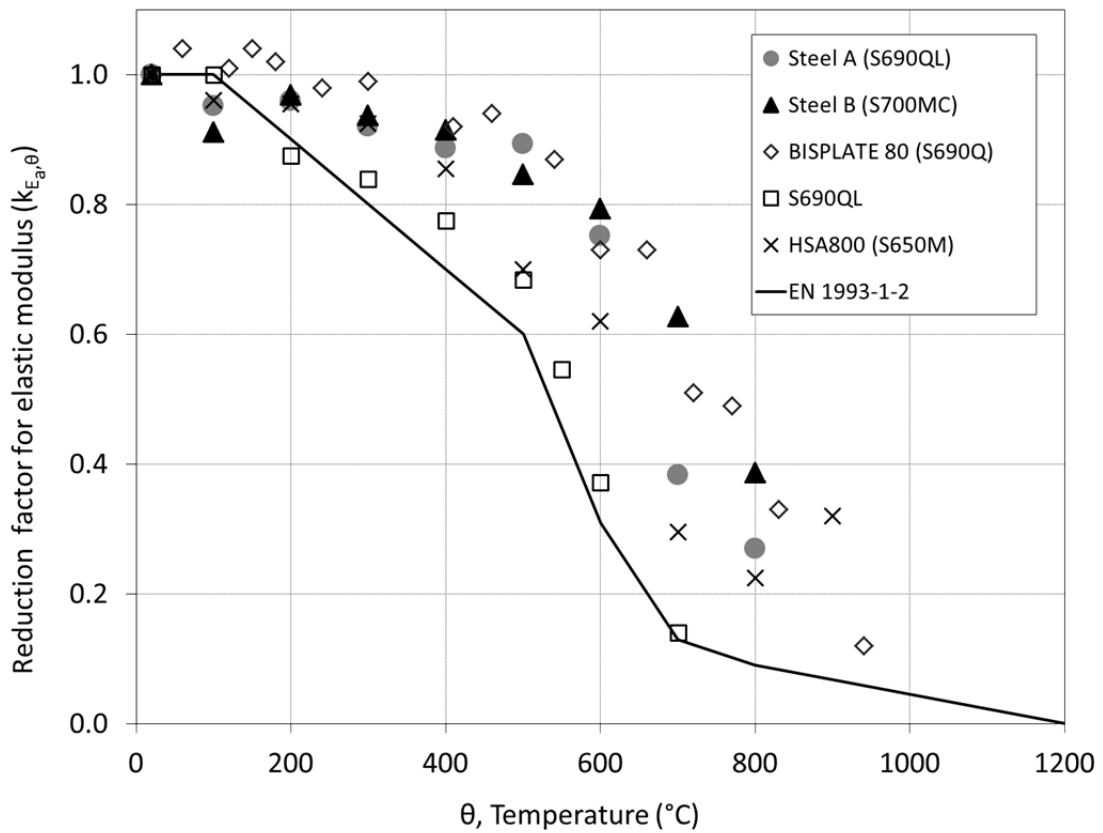
Figure 10: Reduction factors for the 2% yield strength

Figure 11: Reduction factors for the elastic modulus